2019 NDIA GROUND VEHICLE SYSTEMS ENGINEERING AND TECHNOLOGY SYMPOSIUM
POWER & MOBILITY (P&M) TECHNICAL SESSION
AUGUST 13-15, 2019 - NOVI, MICHIGAN

FUNDAMENTAL STUDY ON THE SUPPRESSION OF DENDRITE GROWTH IN LITHIUM-METAL BATTERIES VIA CARBON NANORIBBONS THROUGH IN-SITU OPTICAL MISCROSCOPY

David Skalny[1], James Mainero[1], Elise Joseph[1], Michael Anger[2], Bradley Fahlman[2]

[1]Combat Capabilities Development Command (CCDC) Ground Vehicle Systems Center (GVSC), Warren, MI

[2]Central Michigan University, Mount Pleasant, MI

ABSTRACT

The purpose of this project was to study the underlying fundamental phenomena associated with the formation of dendrites in Lithium-metal batteries through the use of in-situ optical microscopy, and other techniques, and develop material solutions to suppress dendritic growth, such as carbon (graphene) nanoribbons (CNRs). Throughout the course of this effort, sixteen different slurry compositions were prepared and made into a total of 96 electrodes (six of each composition). These electrodes were built into in-situ optical cells and coin half-cells and then tested using in-situ optical microscopy and cycle testing. The results found that the inclusion of CNRs generally reduced the severity of dendrite formation.

Citation: D. Skalny, J. Mainero, E. Joseph, M. Anger, B. Fahlman, "Fundamental Study on the Suppression of Dendrite Growth in Lithium-Metal Batteries via Carbon Nanoribbons Through In-Situ Optical Microscopy", In *Proceedings of the Ground Vehicle Systems Engineering and Technology Symposium* (GVSETS), NDIA, Novi, MI, Aug. 13-15, 2019.

1. INTRODUCTION

The military requires batteries to provide energy and power for starting, lighting, & ignition, Silent Watch, and Silent Mobility. As energy demand continues to grow as more sophisticated electronics are added to the fleet. Current and future Army ground-vehicle demands for increased electrical power, longer silent operation, reduced weight and improved battery durability have driven the Ground Vehicle Systems Center's (GVSC's) development of next generation battery technologies. Unfortunately, Lithium-ion battery chemistries have insufficient theoretical capacity to achieve the level of storage required for significant further increases in energy density. Additionally, to

support future vehicle concepts, such as an all-electric tank, batteries with significantly higher energy densities, such as Lithium-metal batteries are required. Lithium-metal battery technology offers a much higher theoretical capacity (3,842 mAh/g) than existing Lithium-ion cell chemistries, nearly 10 times, making it a promising solution for emerging needs. [4] However, Lithium-metal batteries have issues with both cycle life and safety that need to be studied and addressed because Lithium metal suffers from the formation of dendrites which can lead to electrical shorting between the cathode and anode. [4] Lithium-metal battery cycle life and safety deficiencies are therefore directly attributable to dendritic growth.

2. BACKGROUND

Dendrites form in the subsurface of Lithium-metal, and the volume extending from the surface is on the same order as that protruding into the electrode. [4] Because Lithium-metal is lacking in "pores or networks that can entrap dendrites that are formed in the subsurface … the dendritic projections are free to penetrate out of the surface and into the electrolyte, leading to potential shorting hazards." [4] One of the most promising strategies for the suppression of dendritic growth in Lithium-metal batteries is through the use of nanoscale materials, including carbon materials. [6, 7] There are various research efforts being performed on the study of Lithium dendrites as well as on the study of Lithium dendrite inhibition through different techniques. In *Mukherjee*, a porous graphene network was used to entrap Lithium-metal like a sponge, which in turn prevented dendritic growth, resulting in very high specific capacity and excellent cycle life. [4] In *Lu*, Lithium dendrite formation was inhibited through the use of a copper nanowire network which trapped Lithium-metal in a 3D nanostructure. [6] In *Zheng*, Lithium-metal coated with interconnected amorphous hollow carbon Nano-spheres was found to prevent dendrite growth. [7] Finally, in *Sun*, the capacity limit of graphite anodes was overcome by reversibly plating Lithium-metal into the space between artificial graphite particles. [5]

In terms of directly studying the growth and suppression of dendrites, in-situ optical microscopy is a powerful tool for real-time observation. [1, 2]

Additionally, carbon nanoribbons have been used as an intercalation material or a conductive additive in Lithium and Lithium-ion batteries. [3, 8]

3. PROJECT DESCRIPTION

This project focuses on the fundamental study of carbon nanoribbons (CNRs) as a potential dendrite suppressant in Lithium-metal batteries. The first objective was to study fundamental phenomena associated with the growth of dendrites in Lithium-metal batteries through in-situ optical microscopy at various charge/discharge conditions. The second objective was to develop methods for application of CNRs to Lithium metal in order to provide a barrier to dendritic growth. Finally, the effectiveness of CNRs in the suppression of the growth of dendrites was quantified and assessed through the use of in-situ optical microscopy.

In-situ optical microscopy, electrochemical impedance spectroscopy (EIS), and cyclic voltammetry (CV) are the best approaches to study dendrites as they form in real-time, and these methods have been or will be applied in this project. In terms of material-based solutions to suppress dendrite formation in Lithium-metal batteries, carbon-based, nanoscale/nanostructured materials have produced impressive specific capacity and cycle life results. As part of a past GVSC project with Central Michigan University (CMU), carbon nanoribbons were researched as an intercalation Lithium-ion battery anode material and several vials of CNR material were provided to GVSC for use in cell-level testing. This project examines if a battery electrode constructed from CNRs will exhibit similar beneficial characteristics as seen in other carbon-based nanoscale materials which have

performed as a barrier to dendritic growth in Lithium-metal cells by forming a network of CNRs to allow for plating/deposition of metallic Lithium into the material without formation of dendrites through entrapment. CNRs also have good electrical conduction, a property which is beneficial for quick transfer of electrons to cell current collectors.

The formation of Lithium metal dendrites was assessed using in-situ optical microscopy and time-lapse photography and quantified based on number, rate of growth, shape, directionality, length, and diameter as well as based on time of formation and location of formation. This analysis allows determination of the impact of CNRs on the rate of dendrite formation. Cell charge & discharge cycling data, including capacity, is also being analyzed to determine energy & power densities as well as cycle-ability (cycle life). The data being collected for this project is principally laboratory experimental data, including cell cycling data (voltage, current, and capacity) and time-lapse photographs of dendrite formation using a microscope with camera.

4. EXPERIMENTAL SETUP

This section describes the materials used in the construction of cells for testing under this project as well as the in-situ optical microscopy test apparatus developed to take time-lapse photography for analysis of real-time dendrite formation.

4.1. Electrode Compositions

Sixteen electrode compositions were studied under this project to determine the effect of varying amounts of CNRs on the formation of dendrites in Lithium-metal and Lithium-ion-based battery cells. These electrode blends are listed in Table 1 below. All of the blends contain 10% PVDF binder by weight. Blends #1-4 were developed as test controls and represent electrodes made of a single material, either Mesocarbon Microbeads (MCMB), Artificial Graphite (AG), or CNRs, typically with Carbon Black (CB). In blends where CNRs were present, electrode compositions were made both with (5% by weight) and without CB additive as CNRs are also conductive and electrodes incorporating CNRs may not require CB. All powders were obtained from MTI Corp., with the exception of the CNRs which were obtained from a previous project with CMU. They have the following part numbers: Artificial graphite powder (EQ-Lib-CMSG), PVDF Binder (EQ-Lib-PVDF), MCMB Powder (EQ-Lib-MCMB), and CB (EQ-Lib-SuperP).

Blend#	MCMB	AG	CNR	CB	PVDF
1	85	-	-	5	10
2	-	85	-	5	10
3	-	-	85	5	10
4	-	-	90	-	10
5	75	-	10	5	10
6	-	75	10	5	10
7	80	-	10	-	10
8	-	80	10	-	10
9	65	-	20	5	10
10	-	65	20	5	10
11	70	-	20	-	10
12	-	70	20	-	10
13	55	-	30	5	10
14	-	55	30	5	10
15	60	-	30	-	10

16	-	60	30	-	10

Table 1: Electrode Compositions by Weight Percentage

4.2. Electrode SEM Images

Scanning Electron Microscope (SEM) images were taken of one set of sixteen electrodes representing the sixteen electrode compositions studied under this project. The images were taken to get a general understanding of the electrode microstructures formed by the combination of the various materials. It is important to note, that due to equipment limitations, the images taken were not of sufficient resolution to see individual CNRs. Four sample SEM images, representing the three controls (MCMB-only, CNR-only, and AG-only) as well as a multi-material blend (MCMB+CNRs) are shown in the images below (see Figure 1).

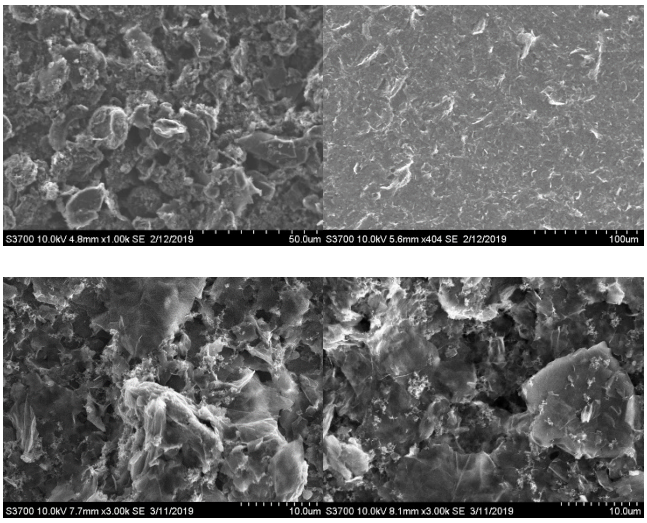

Figure 2: Sample SEM Images (Upper Left: MCMB Control, Upper Right: CNR Control, Lower Left: AG Control, Lower Right: MCMB/CNR Blend)

4.3. Slurry Preparation

Sixteen slurries were prepared according to the electrode composition blends defined in the previous section. First the individual powders (MCMB, AG, CNR, and CB) were weighed to achieve the desired mass percentages required to make the sixteen different slurry compositions. PVDF powder was then weighed to serve as a binder for the electrode powders. NMP solvent was added to the binder to dissolve the PVDF and prepare it for combination with the powder blends. Milling balls were added to the binder to aid in the vortex mixing/ball milling processes. The mixture was briefly heated on a hot plate as needed to aid in melting and solvation of the PVDF. The powder blends were subsequently added to the solvated PVDF binder. The slurry was then ball milled using a vortex mixer until the proper consistency was achieved. Additional NMP was added incrementally if necessary to achieve this consistency.

4.4. Electrode Fabrication

Copper disks were punched from copper foils and weighed to create current collectors for the electrodes. The copper foil used had been stored under vacuum seal to prevent tarnishing. The sixteen slurries were then applied to the copper disks using a painting technique. The electrodes were then vacuum dried and weighed to allow determination of active material mass. The dried electrodes were sorted into marked containers for later insertion into in-situ optical or coin cells, SEM imaging, or long-term storage.

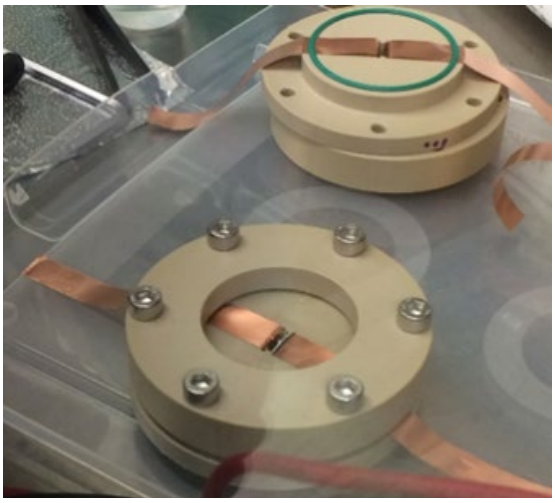

Figure 1: MTI Corp. PEEK Cell

A total of ninety-six electrodes were fabricated at GVSC for use in testing as part of this project (6

electrodes each of each of the sixteen material compositions). Of these 96 electrodes, one set was used for SEM imagery (electrodes were preserved to the extent possible and used to build additional coin cells), two sets were used/reserved for in-situ optical microscopy, two sets were used for coin half cells, and one set was reserved for future use in Lithium-ion full cells.

4.5. Cell Assembly

The prepared coated anodes were pre-inserted into the in-situ optical cells prior to final assembly in the Argon glovebox. Inside the glovebox, the Lithium foil was inserted on a copper backing into the in-situ optical cell electrode opening. Electrolyte was added to each well and the cell was sealed. Additionally, a total of forty-three coin half cells were built (five were found to be non-functional) using three sets of the sixteen different electrode compositions. These coin half cells are currently on test using a MACCOR coin cell cycler at CMU for cycle life and capacity analysis.

4.6. In-Situ Optical Cell

In-situ optical analysis was performed on sixteen of the ninety-six GVSC-fabricated electrodes to characterize Lithium-metal deposition and dendrite formation on both the Lithium metal reference electrode and the carbon-based electrode materials. Initial experiments for this project were conducted with in-situ optical cells from MTI Corp.: PEEK Split Cells with Quartz Window for In-Situ Optical Microscope Analysis (EQ-STC-PQW) (see Figure 2). However, due to limitations in cycle life found using these cells and limited experimental throughput, a customized GVSC cell was developed and was used to collect the data presented herein. For the purposes of the in-situ optical analysis, only eight material compositions were selected from the sixteen developed, which included the MCMB and CNR control electrodes as well as the MCMB & CNR blends with carbon black. Two electrodes of each composition were tested and analyzed using the in-situ optical test apparatus. The additional eight material compositions were not subjected to in-situ optical analysis, as the structure were deemed likely to produce similar results to those acquired through testing the first eight compositions. However, these compositions are being subjected to electrochemical analysis and cycling in the form of coin half cells.

4.7. In-Situ Optical Cell Test Apparatus

The in-situ optical cells were tested using a custom testing apparatus built by GVSC for in-situ optical microscopy (see Figure 3). This testing apparatus consisted of a modified ARMAG steel enclosure with CO_2 fire suppression system, a Meiji EMZ-13TR stereo zoom microscope, a Techniquip F150-1K6X-TQP illuminator, a 32-inch Samsung HDTV, a Nikon D5600 camera, a MTI Corp. BST8-WA 8 Channel Battery Analyzer (0.005-1mA, 5V), and a MTI Corp. BST8-MA 8 Channel Battery Analyzer (0.02 -10 mA, 5V).

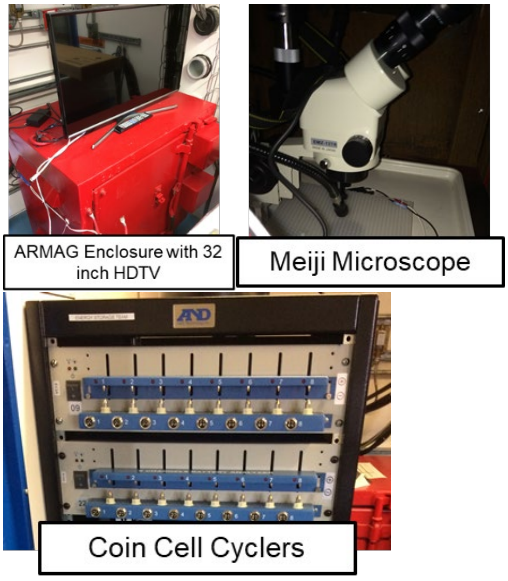

Figure 3: Custom In-situ Optical Microscopy Test Apparatus

5. RESULTS

This section describes the cycling performed on the in-situ optical cell and the observations resulting from this cycling. From the collection of electrodes that were produced, two sets of eight electrodes were built into the optical cell to be cycled and observed for dendritic formation. For this purpose, only electrode designs using MCMB, CNR, and their blends as active materials were used. These electrodes are identified in the table below:

Electrode	MCMB%	CNR%	CB%	PVDF%
1st Set				
E05	85	0	5	10
E17	0	85	5	10
E30	75	10	5	10
E41	80	10	0	10
E53	65	20	5	10
E65	70	20	0	10
E78	55	30	5	10
E89	60	30	0	10
2nd Set				
E06	85	0	5	10
E18	0	85	5	10
E29	75	10	5	10
E42	80	10	0	10
E54	65	20	5	10
E66	70	20	0	10
E77	55	30	5	10
E90	60	30	0	10

Table 2: Optical Cell Electrode selection

Formation cycles of 1 mA per cell were performed prior to attempting to induce the formation of dendrites on the carbonaceous electrodes. Unless otherwise noted, cells were cycled between 0V and 3V.

5.1. High power cycling

There are two basic strategies which can be implemented when cycling cells to induce Lithium-ion dendrite growth. Both strategies were attempted during this experiment. The first method is to cycle the battery cell at high current rates. If a high enough current is used, the ability of the carbonaceous electrode material to intercalate Lithium ions will be overwhelmed, resulting in Lithium plating or dendrite formation on the surface of the material. To accomplish this, the 1st set of cells were cycled at incrementally increasing currents from 6 mA to 18 mA. During this cycling, significant pitting and dendrite formation was readily observed on the Lithium-metal counter electrode. However, little to no plating was observed on the experimental carbonaceous electrode and the behavior could not be well correlated to the electrode designs. This high current approach could be improved by attempting cycling at lower temperatures, but the experimental apparatus was not able to be implemented in a temperature controlled environment. Therefore, a second method was attempted to induce dendrite formation.

5.2. Overdischarging

The same cells made from the 1st set of electrodes were fully discharged at a rate of 1 mA to 0V, such that the maximum amount of Lithium was moved into the carbonaceous electrode via a normal cycle. After this discharge, the polarity of the cycler equipment was reversed, so that a voltage of -0.5V could be applied in order to drive more Lithium into the carbonaceous electrode. A current of 0.5 mA

was applied to each cell at this voltage at a continuous rate for each cell. Using this method, Lithium was successfully plated onto all of the electrodes in the 1st set, except for E89 (E89 was unable to maintain the 0.5 mA discharge rate and may be a defective cell). The point of onset of Lithium plating/dendrite formation was then identified visually using the video recorded by the microscope and camera during this process and converted to a number of minutes of cycle time. Normalizing this number by the mass of each electrode allows the trend in the ability of the electrode blend to inhibit dendritic growth to be observed. This process was repeated with the 2nd set of electrodes to provide an additional data point for each blend, skipping the high power cycling described in section 5.1. This data is summarized in the table below:

%MCMB/CNR/CB/PVDF	1st Set	2nd Set
85/0/5/10	42	138
0/85/5/10	105	120
75/10/5/10	63	177
80/10/0/10	120	177
65/20/5/10	81	141
70/20/0/10	90	132
55/30/5/10	63	183
60/30/0/10	-	135

Table 3: Lithium plating/dendrite onset time weighted by electrode mass (min/mg)

5.3. Analysis

Electrode	Observations
1st set	
E05	Gold intercalation. Thick uniform Li plating
E17	Localized jagged dendrites
E30	Uniform Li plating
E41	Uniform Li plating
E53	Uniform Li plating
E65	Uniform Li plating
E78	Uniform Li plating
E89	Cell could not maintain current during overcharge
2nd set	
E06	Gold intercalation. Thick uniform Li plating. Discharge rate decayed.
E18	Localized jagged dendrites
E29	Few localized large dendrites
E42	Uniform Li plating
E54	Uniform Li plating
E66	Uniform Li plating
E77	Non-uniform Li plating. Discharging rate decayed.
E90	Uniform Li plating

Table 4: Visually observed electrode behavior

The visually observed behavior of each electrode is summarized in the table above. The behavior of the electrodes during cycling can generally be divided into three broad categories. The electrodes based on pure MCMB active material turned a golden color as they became fully intercalated with Lithium. As additional Lithium is driven into the electrode, a fairly uniform layer of silver colored

Lithium forms over the electrode and slowly increases in thickness. The image below shows an example of a pure MCMB electrode at the onset of Lithium plating and at the end of the overdischarge.

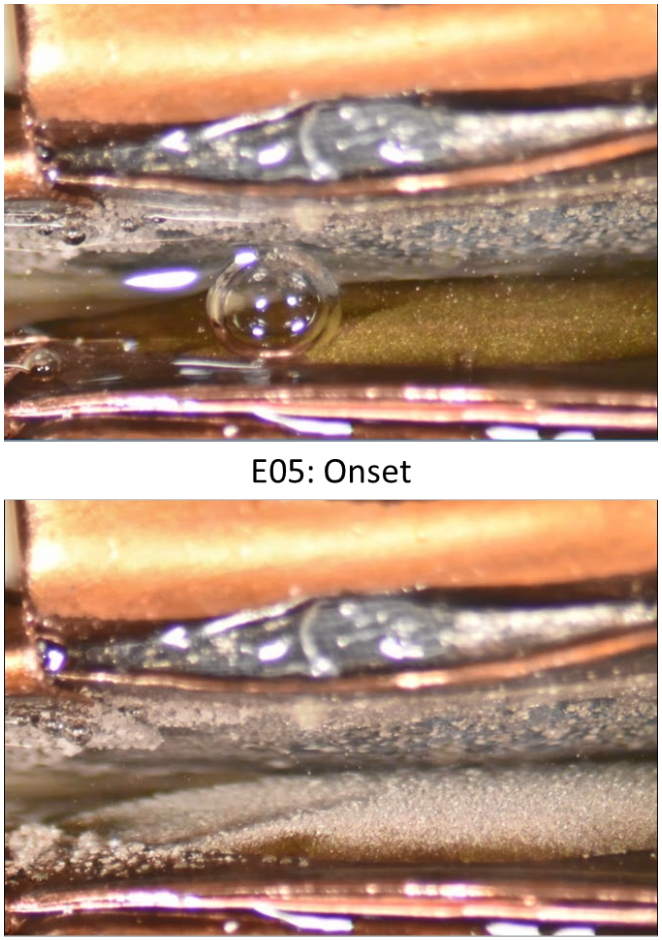

Figure 4: Pure MCMB electrode (E05)

In contrast, the electrode made with pure CNR active material form jagged dendrites which protrude from localized nucleation points.

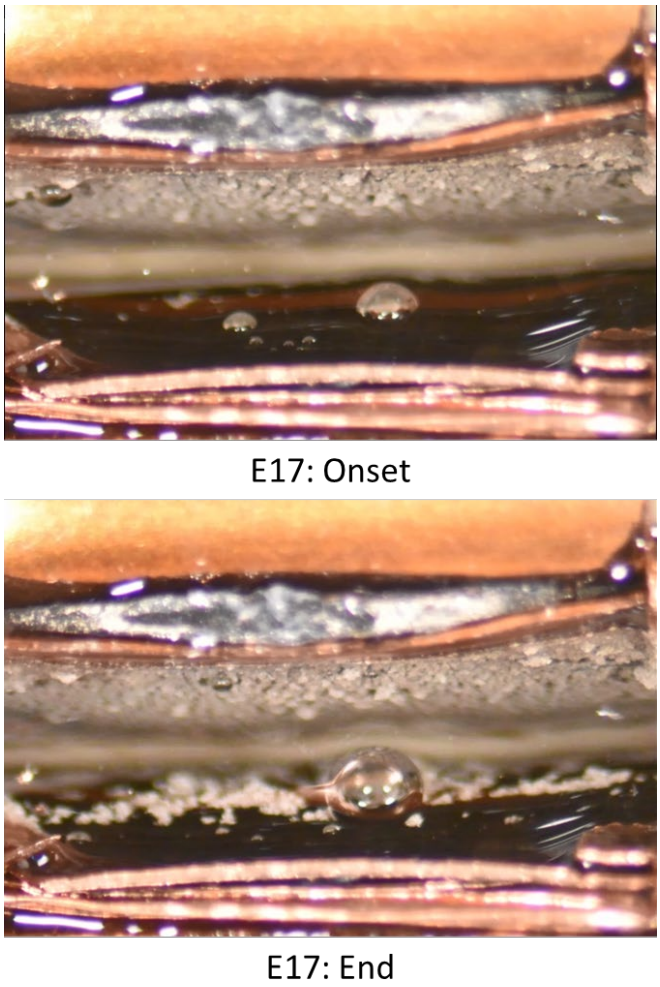

Figure 5: Pure CNR electrode (E17)

Lastly, in most cases the blended MCMB and CNR electrodes also plate Lithium uniformly over the electrode. However, they do not exhibit the characteristic gold intercalation color of the pure MCMB and the Lithium layer on top of the electrode appears less thick, perhaps indicating more Lithium has been hosted internal to the carbonaceous structure.

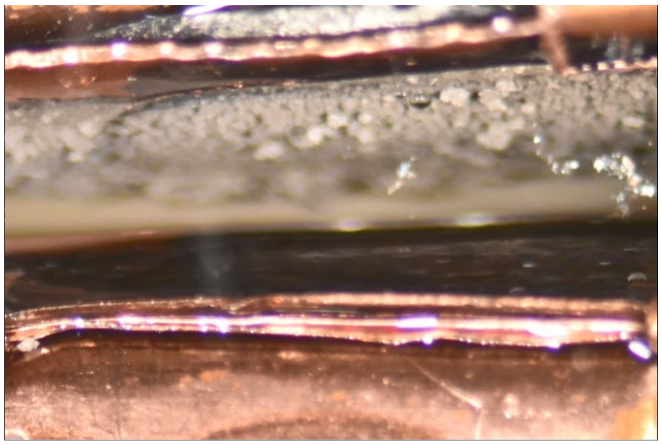

E41: Onset

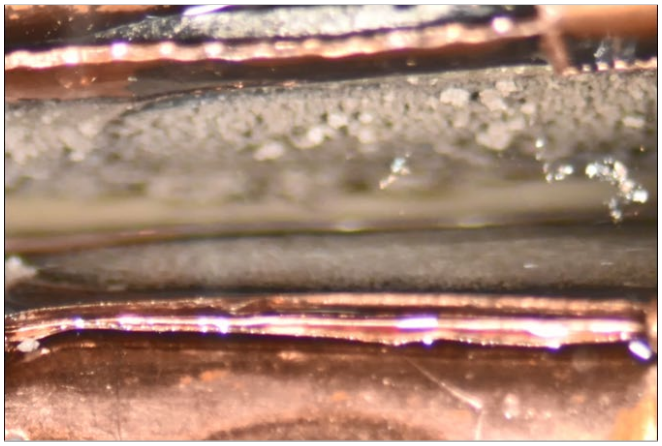

E41: End

Figure 6: MCMB/CNR blend electrode (E41)

Based on the normalized onset times of plating/dendrite formation during the over discharge experiments, it was possible to observe trends in the ability of each electrode composition to inhibit Lithium plating/dendritic growth. This is plotted in figure 7. It was observed that the pure CNR composition is able to uptake more Lithium than the MCMB composition. However, as shown in Figures 4 and 5, the type of dendrites formed on the CNR composition protrude much further and are much more localized than the uniform plating of the MCMB. This is an undesirable outcome, as these type of dendrites may be more likely to penetrate through the separator in a full battery cell, resulting in shorting between the electrodes, despite the delayed onset.

For the blends, the onset of plating/dendrites is more inhibited than for pure MCMB as indicated by their longer onset times, but they also exhibit the more favorable uniform plating in most cases. As the percent of CNR in the electrode composition is increased from 10% to 30%, a general trend of increased onset time is observed. Further, for each electrode pair with the same CNR percent composition, the electrode with carbon black exhibited slightly longer onset times than the electrode without carbon black. This may indicate carbon black also plays a role in Lithium plating/dendrite suppression.

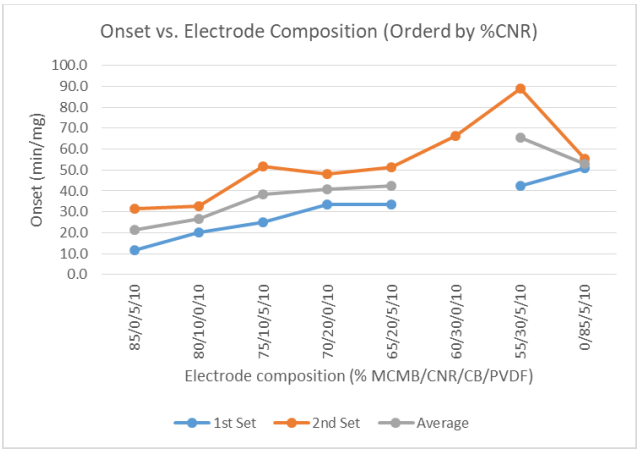

Figure 7: Lithium Plating/Dendrite Onset

6. CONCLUSIONS

Based on the trends observed, blending CNR material into MCMB or other carbonaceous anode materials may result in an electrode structure which inhibits Lithium plating/dendrite formation. Further, while the use of CNRs may also enable the elimination of carbon black from the electrode due to their intrinsic conductivity, keeping CB in the electrode composition appears to further reduce Lithium plating/dendrite formation.

7. ACKNOWLEDGEMENTS

We would like to thank our Cooperative Research & Development Agreement (CRADA) partner, Dr. Bradley D. Fahlman and his team at Central Michigan University (Jonathon Clapham, Michael Anger) for their support in the continuation of this important research under the GVSC-CMU CRADA "Novel Carbonaceous Materials for Lithium Battery Improvement" as well as our GVSC colleagues who assisted us in the development of the tools required to complete the initial phase of this project.

8. REFERENCES

[1] K. Wood, et al., "Dendrites and Pits: Untangling the Complex Behavior of Lithium Metal Anodes through Operando Video Miscroscopy," ACS central science, vol. 2.11, pages 790-801, 2016.

[2] W. Li, et al., "The synergetic effect of Lithium polysulfide and Lithium nitrate to prevent Lithium dendrite growth," Nature communications, vol. 6, page 7436, 2015.

[3] T. Bhardwaj, et al., "Enhanced electrochemical Lithium storage by graphene nanoribbons," Journal of the American Chemical Society, vol. 132.36, pages 12556-12558, 2010.

[4] R. Mukherjee, et al., "Defect-induced plating of Lithium-metal within porous graphene networks," Nature communications, vol. 5, page 3710, Apr. 2014.

[5] Y. Sun, et al., "Graphite-encapsulated Li-metal hybrid anodes for high-capacity Li batteries," Chem, vol 1.2, pages 287-297, 2016.

[6] L. Lu, et al., "Free-standing copper nanowire network current collector for improving Lithium anode performance," Nano letters, vol. 16.7, pages 4431-4437, Jun. 2016.

[7] G. Zheng, et al., "Interconnected hollow carbon nanospheres for stable Lithium-metal anodes," Nature nanotechnology, vol 9, pages 618-623, Aug. 2014.

[8] T. Wang, et al., "Ultrafast charging high capacity asphalt-lithium metal batteries," ACS nano, vol. 11.11, pages 10761-10767, 2017.